

Web bend-buckling strength of plate girders with two longitudinal web stiffeners

Byung Jun Kim^{1a}, Yong Myung Park^{*1}, Kyungsik Kim^{2b} and Byung H. Choi^{3c}

¹Dept. of Civil Engineering, Pusan National University, Busan 46241, Republic of Korea

²Dept. of Civil Engineering, Cheongju University, Cheongju 28503, Republic of Korea

³Dept. of Civil Engineering, Hanbat National University, Daejeon 34158, Republic of Korea

(Received November 26, 2018, Revised December 19, 2018, Accepted January 21, 2019)

Abstract. More than one longitudinal web stiffener may be economical in the design of plate girders that have considerably high width-to-thickness ratio of webs. In this study, the bend-buckling strength of relatively deep webs with two horizontal lines of flat plate-shaped single-sided stiffeners was numerically investigated. Linear eigenvalue buckling analyses were conducted for specially selected hypothetical models of stiffened web panels, in which top and bottom junctions of a web with flanges were assumed to have simply supported boundary conditions. Major parameters in the analyses were the locations of two longitudinal stiffeners, stress ratios in the web, slenderness ratios and aspect ratios of web panels. Based on the application of assumptions on the combined locations of the two longitudinal web stiffeners, simplified equations were proposed for the bend-buckling coefficients and compared to the case of one longitudinal stiffener. It was found that bend-buckling coefficients can be doubled by adopting two longitudinal stiffeners instead of one longitudinal stiffener. For practical design purposes, additional equations were proposed for the required bending rigidity of the longitudinal stiffeners arranged in two horizontal lines on a web.

Keywords: plate girder; stiffened web; two longitudinal stiffeners; web bend-buckling strength; bending rigidity of stiffener

1. Introduction

In most design practice, plate girders may be proportioned to have highly slender webs for economic reasons as the section design of plate girders is typically governed by bending moments rather than shear forces. The width-to-thickness ratios of the web, however, must be properly controlled to prevent the web bend-buckling, an elastic buckling of the web due to bending moment, that can result in a considerable decrease in the flexural strength (Cooper 1967). Longitudinal stiffeners are commonly used to prevent a premature bend-buckling by controlling the out-of-plane deformation of the webs. In addition, stiffened webs can provide improved rotational restraint to the compression flanges and consequently result in increased bending resistance (Ziemian 2010, Park *et al.* 2016).

Fig. 1 shows the schemes of stiffened webs with flat plate-shaped single-sided stiffener(s), which are used in practical design of plate girders. Many researches have been conducted for the buckling strength of the stiffened webs

with one stiffener (Alinia and Moosavi 2008, Azhari and Bradford 1993, Cho and Shin 2011, Dubas 1948, Frank and Helwig 1995, Issa-EI-Khoury *et al.* 2014, Maiorana *et al.* 2011, Massonnet 1954, Rockey 1958, Rockey and Leggett 1962, Kim *et al.* 2018). Of these, Frank and Helwig performed a series of eigenvalue analysis for the optimum location of the longitudinal stiffener, in which the top and bottom junctions of the web were assumed to be simply supported. Based on their study, they reported that the optimum location of the single stiffener could be expressed as $d_s/D_c = 0.4$, regardless of the asymmetry of the girder section, where d_s and D_c are the distance between the stiffener and the compression flange, and the depth of the web in compression in the elastic range, respectively. The equations for buckling coefficients of the stiffened webs were proposed separately for cases when $d_s/D_c \geq 0.4$ and $d_s/D_c < 0.4$, which have been adopted by the current AASHTO LRFD bridge design specifications (AASHTO 2017).

With the advent of high-strength steels, the span length of plate girder bridges becomes longer. Accordingly, the web depth becomes higher to satisfy flexural strength and control vertical deflection. In such a deep web, two or more longitudinal stiffeners could be required to prevent the bend-buckling of the web. However, the research on the web panels stiffened with two lines of longitudinal stiffeners are very limited. Rockey and Cook (1965a) conducted a study on the bend-buckling strength of the web stiffened with two longitudinal stiffeners for doubly-symmetric section. They assumed that the flanges provided either a simple support or a clamped support while the

*Corresponding author, Professor
E-mail: ympk@pusan.ac.kr

^aPh.D. Student
E-mail: bjun1300@pusan.ac.kr

^bAssociate Professor
E-mail: kkim@cju.ac.kr

^cAssociate Professor
E-mail: bhchoi@hanbat.ac.kr

transverse stiffening results in a simple support. It was also assumed that the longitudinal stiffeners were symmetrically placed, i.e., double-sided, about the mid-plane of the web and their bending rigidity was finite but torsional rigidity was negligible. Based on the energy method, they concluded that the most effective combination of positions for the stiffeners are at $0.136D$ and $0.284D$ from the compression flange, and a buckling coefficient (k) of 356 is obtained for clamped webs, in which D is the depth of the web. When the junctions of the web and flange are simply supported, the corresponding values are $0.123D$, $0.275D$ and 313, respectively.

Rockey and Cook (1965b) also proposed an approximate method for the solutions of the web bend-buckling strength reinforced with multiple stiffeners for doubly-symmetric section. The buckling strength of the sub-panels were computed by treating them as individual rectangular plates, assuming that the longitudinal stiffeners provide simple supports. Clearly, this would be a lower bound to the actual buckling strength since it neglects any ‘continuity effect’ at the location of the stiffeners. It was considered that the stiffeners are located at the optimum locations when all sub-panels exhibit the same buckling strength. Based on the proposed method for the webs with two stiffeners, optimum combined positions and corresponding k value were proposed as $0.139D$, $0.289D$ and 319 for clamped webs and $0.129D$, $0.283D$ and 293 for simply supported webs, respectively. It was assumed in their study that all of the longitudinal stiffeners have same size and approximate equations for the bending rigidity of the double-sided longitudinal stiffeners, that is required for the formation of ‘nodal line’, were proposed for simply supported and clamped conditions.

The AASHTO LRFD bridge design specification does not specify the bend-buckling coefficient of the webs with two longitudinal stiffeners separately and stipulates that the buckling coefficient for singly-stiffened webs can be used conservatively. Alternatively, the engineers are permitted to determine the buckling coefficient by direct buckling analysis of the web panels with multiple stiffeners, in which the boundary conditions at the flanges and at the stiffener locations should be assumed as simply supported. However, the maximum slenderness ratio of the stiffened web is limited to be less than 300, regardless of the number of the stiffeners. This provision could result in an uneconomical design of plate girders with more than one stiffener, especially in deep girders.

The main purpose of this study is to propose practical equations for determining the bend-buckling coefficients of web panels stiffened with flat plate-shaped single-sided two longitudinal stiffeners as shown in Fig. 1(b) in doubly- and mono-symmetric section plate girders subjected to in-plane bending. The stiffened web panel was assumed as a single plate with simple support conditions that is the same schematics as AASHTO LRFD specifications. Comprehensive eigenvalue analyses were conducted for a quantitative evaluation of the buckling coefficients. The major parameters in this study include the combined locations of two stiffeners, stress ratios in the web, slenderness ratios and aspect ratios of web panels. In

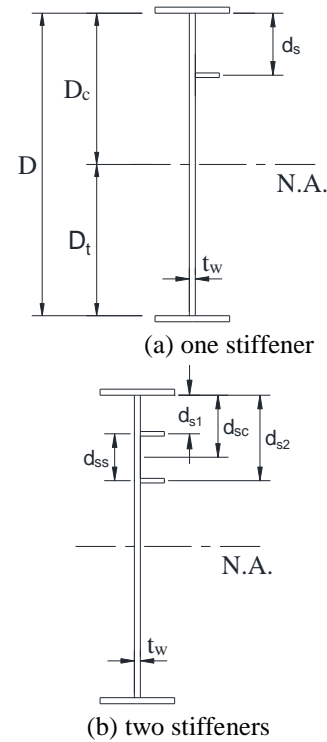


Fig. 1 Stiffened web with flat plate-shaped single-sided longitudinal stiffener(s)

addition, requirements for the bending rigidity of the longitudinal stiffeners to appropriately suppress the web bend-buckling, i.e., to form nodal lines, in terms of the aspect ratios were analyzed.

2. Code provisions for web bend-buckling strength

2.1 AASHTO LRFD specifications

In the AASHTO LRFD specifications (AASHTO 2017), the nominal bend-buckling strength of a web (F_{crw}), which is based on the theoretical plate buckling strength (Bleich 1952, Timoshenko and Gere 1963), is expressed as follows

$$F_{crw} = \frac{0.9kE}{\left(\frac{D}{t_w}\right)^2} \tag{1}$$

where, k is the bend-buckling coefficient, and E is the elastic modulus of steel. Along with Eq. (1), Eq. (2a) presents the limit of the slenderness ratio of stiffened webs at which F_{crw} reaches the yield strength of the compression flange, F_{yc} .

$$\frac{D}{t_w} \leq 0.95 \sqrt{\frac{kE}{F_{yc}}} \tag{2a}$$

$$D/t_w \leq 300 \tag{2b}$$

The stiffened webs that satisfy Eq. (2a) are considered effective through the whole depth until the yield moment is

reached, i.e., they are regarded as noncompact webs. In addition, AASHTO LRFD specifications limit the slenderness ratio of the stiffened webs to be less than 300 as given in Eq. (2b).

As stated previously, the buckling strength for the web with one stiffener in the AASHTO was originated from Frank and Helwig (1995). Based on their numerical analyses on the simply supported stiffened webs, the buckling coefficient equations were proposed as follows.

$$d_s/D_c < 0.4 : k = \frac{11.64}{\left(\frac{D_c - d_s}{D}\right)^2} \quad (3a)$$

$$d_s/D_c \geq 0.4 : k = \frac{5.17}{\left(\frac{d_s}{D}\right)^2} \quad (3b)$$

AASHTO LRFD specifications stipulate that Eq. (3) can be used conservatively for webs with more than one longitudinal stiffener, and no other specific equations are provided for the web with two or more stiffeners.

2.2 Eurocode 3

EN 1993-1-5 of Eurocode 3 (CEN 2006) specifies that the bending resistance of girder sections can be determined by considering the effective widths of the stiffened web and the compression flange, which are dependent on the buckling strengths of the plate elements. It must be noted that the buckling coefficients are determined based on the assumption of simply supported conditions along the edges of individual sub-panels divided by the longitudinal stiffeners and/or the flanges. For a stiffened web, the Equations for bend-buckling coefficient are defined as a function of the stress ratio (ψ) for a sub-panel and given for three ranges

$$\begin{aligned} k &= 8.2/(1.05 + \psi) \text{ for } 0 < \psi < 1 \\ k &= 7.81 - 6.29\psi + 9.78\psi^2 \text{ for } -1 < \psi < 0 \\ k &= 5.98(1 - \psi)^2 \text{ for } -3 < \psi < -1 \end{aligned} \quad (4)$$

where, ψ is the stress ratio of the upper edge to the lower edge at the corresponding sub-panel.

These assumptions in Eurocode 3 will provide a lower bound of buckling strengths due to ignoring the 'continuity effect'. Eq. (4) gives k values of 300.4, 285.8 and 262.5 converted from the upper, middle and lower sub-panel, respectively, when the stiffeners are placed at the optimum locations, $0.123D$ and $0.275D$ in the doubly-symmetric simply supported web panel. Considering the k value as 313 in the isolated single web panel under same condition (Rockey and Cook 1965a), Eurocode 3 conservatively estimates the buckling strength of the stiffened web.

The design philosophy for buckling strength stipulated in Eurocode 3 is intrinsically different from that considered in the AASHTO. This study focused on the concept of AASHTO that considers the stiffened web as a single plate panel.

3. Numerical parameters and finite element (FE)

model

3.1 Parameters

Major parameters that could affect the bend-buckling strengths of the stiffened web and their corresponding ranges considered in this study are presented in Table 1.

First of all, a web slenderness ratio, D/t_w , was selected as a variable to investigate the effect of the web slenderness ratio on the buckling strength. Considering $E = 205$ GPa and $k = 313$ in Eq. (2a), the limits of the slenderness ratios are 410 for a conventional steel with $F_{yc} = 345$ MPa (50 ksi) and 290 for a high-strength steel with $F_{yc} = 690$ MPa (100 ksi). Therefore, three different ratios for web slenderness, i.e., 250, 300 and 350 were representatively selected for possible application in practice although AASHTO limits to less than 300. The depth of the web (D) was set as 3,000 mm throughout this study.

The asymmetry of the hypothetical girder sections was considered by the stress ratio $\Psi (= F_t/F_c)$, as shown in Fig. 2, where F_c and F_t are the compressive (positive value) and tensile (negative value) stresses at the junctions of the compression and tension flanges, respectively. The cross-sectional area of the compression flange (A_{fc}) is smaller than that of the tension flange (A_{ft}) in the positive moment zones while A_{fc} is proportioned similar or slightly larger than A_{ft} in the negative moment zones. According to a survey by the authors, most composite plate girder bridges exhibited a range of Ψ value between -0.75 and -1.15 at positive and negative moment sections. The stress ratios in this study were chosen in the range -0.5 ~ -1.5, thus the corresponding D_c is from 2,000 mm to 1,200 mm.

The aspect ratio (α) of the stiffened web is defined as the ratio of spacing of transverse stiffener (d_o) to the web depth (D). As the aspect ratio increases, the dimensions of the longitudinal stiffeners will be larger, which may result in less economical designs with respect to the weight of the material used. In addition, the aspect ratios in practical designs are expected to be smaller than 1.5 as the web depth becomes higher when two longitudinal stiffeners are used. The aspect ratios considered in this study were in the range 0.5~1.5, thus the corresponding d_o is from 1,500 mm to 4,500 mm.

The optimum locations of the stiffeners were determined as $d_{s1} = 0.123D$ and $d_{s2} = 0.275D$ in the doubly-symmetric simply supported web panel (Rockey and Cook 1965a), where d_{s1} and d_{s2} are the distances between the compression flange and the stiffeners as shown in Fig. 1(b), respectively. If the longitudinal stiffeners are located at a fixed distance from the compression flange, which is normally the case, the stiffeners cannot be at their optimum locations throughout the girder. When a single longitudinal stiffener is installed, the optimum location of the stiffener is expressed as the ratio $d_s/D_c (= 0.4)$, regardless of the asymmetry of the sections (Frank and Helwig 1995). Therefore, the location of i^{th} stiffener will be considered by the ratio of d_{si}/D_c . Considering the stress ratio $\Psi = -0.5 \sim -1.5$, the ratios d_{s1}/D_c and d_{s2}/D_c were varied in the range 0.22~0.28 and 0.48~0.68, respectively. Another

Table 1 Major parameters considered in present buckling analysis

Parameter	Range
D/t_w	250, 300, 350 ($D = 3,000 \text{ mm}$)
$\Psi (= F_t/F_c)$	-0.5 ~ -1.5
$\alpha (= d_o/D)$	0.5 ~ 1.5
d_{s1}/D_c	0.22 ~ 0.28
d_{s2}/D_c	0.48 ~ 0.68
d_{sc}/D_c	0.3 ~ 0.5

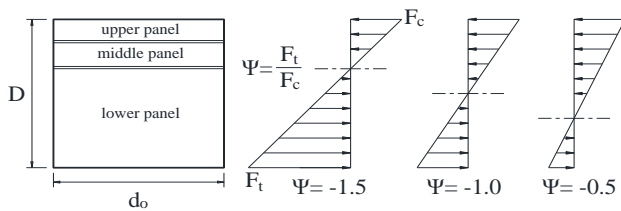
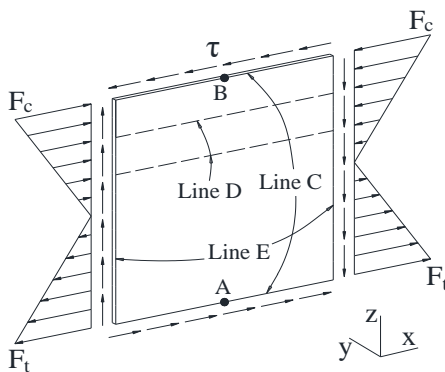


Fig. 2 Stress ratio (Ψ)



Location	Dx	Dy	Dz	Rx
Point A	Fix	-	Fix	-
Point B	Fix	-	-	-
Line C	-	Fix	-	Fix*
Line D, E	-	Fix	-	-

*only for clamped support web

Fig. 3 Scheme of numerical model (Model-I) and boundary conditions

variable, d_{sc}/D_c , is introduced to define the distance between the center of the two stiffeners and the compression flange as shown in Fig. 1(b). This variable will be used to derive the optimum locations of the two stiffeners for practical purposes in Section 4.3, and was varied in the range 0.3 ~ 0.5 to cover the range $\Psi = -0.5 \sim -1.5$.

3.2 Numerical model

The bend-buckling strengths of the stiffened web panels subjected to in-plane bending action were evaluated through

eigenvalue analyses. The scheme of the model and boundary conditions used for the web bend-buckling analysis is shown in Fig. 3. The in-plane bending action of the web plate was simulated with compressive (F_c) and tensile (F_t) stress gradients on both ends of the web. Although present study focuses on the bend-buckling strength of the stiffened web, interactive buckling of the stiffened web under combined in-plane bending and shear is also considered. In this case, the shear stress (τ) was also imposed as shown in Fig. 3.

The upper and lower junctions at the compression and tension flange locations (Line C in Fig. 3) were basically assumed as simply supported conditions according to the AASHTO stipulations. The junctions were restrained from rotation in the selected analysis in order to investigate the influence of the rotational restraints contributed by the flanges on the solutions. The out-of-plane displacements were fixed at the horizontal lines (Line D in Fig. 3) where two longitudinal stiffeners are installed without separately modelling the stiffeners. This FE model will be denoted as ‘Model-I’ to distinguish it from another model which will be shown in Section 5. The transverse stiffeners were not included in the models and both vertical edges of the web (Line E in Fig. 3) were assumed to be simply supported. Such condition may lead subsequent buckling strengths to the conservative side.

The eigenvalue analyses were performed using the ABAQUS software (2018). The S4R 4-node shell elements were employed for modelling the web panels.

3.3 Validation of FE model

Prior to the numerical analyses on the major parameters, some preliminary analyses were conducted to validate the Model-I in Fig. 3. First, convergence tests of the buckling coefficient subjected to in-plane bending were performed under $\Psi = -1.0$ (i.e., doubly-symmetric section) and $\alpha = 1.0$ as the FE mesh was refined. Also, three different web slenderness ratios (D/t_w) of 250, 300 and 350 were considered to investigate the sensitivity of the buckling coefficients according to the web slenderness ratio. As the web depth was set as 3,000 mm, the corresponding web thickness becomes 12 mm, 10 mm, and 8.6 mm. Fig. 4 shows the convergence schemes for the three slenderness ratios of the web panels under simply supported condition, and the difference according to D/t_w is negligible. Based on these results, the web plate was divided into more than 200 elements in depth and the aspect ratio of the shell element was set as close as possible to 1.0.

Secondly, the bend-buckling strength according to the boundary conditions were evaluated under $\Psi = -1.0$, $\alpha = 1.0$ and $D/t_w = 300$. The resultant buckling coefficients for the simply supported(“SS”) and clamped(“CS”) conditions are presented in Fig. 5(a) and Table 2. In the analysis, the location of the upper stiffener was assumed at $0.246D_c (= 0.123D$ when $\Psi = -1.0$) for SS and $0.272D_c (= 0.136D$ when $\Psi = -1.0$) for CS condition, which are the optimum locations suggested by Rockey and Cook (1965a). The location of the lower stiffener was varied between $0.5D_c$ and $0.68D_c$. The theoretical values

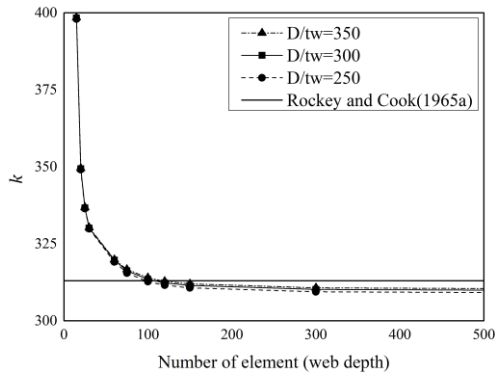
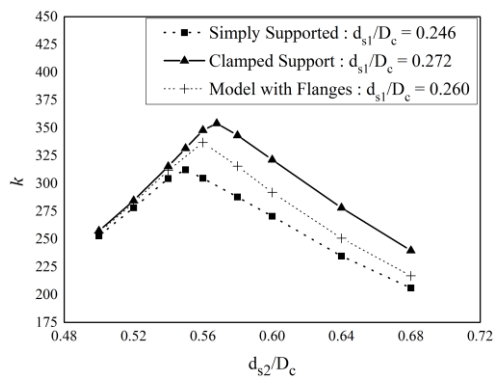
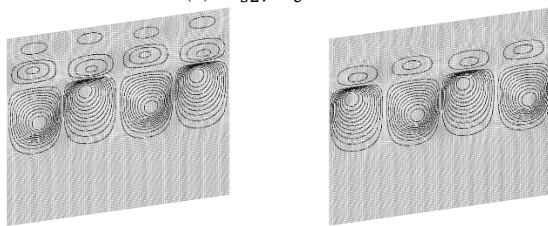


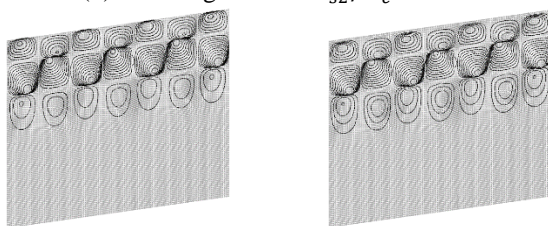
Fig. 4 Mesh convergence tests: simply supported web ($\Psi = -1.0$, $\alpha = 1.0$)



(a) d_{s2}/D_c vs. k



SS web CS web
(b) Buckling modes: $d_{s2}/D_c = 0.54$



SS web CS web
(c) Buckling modes: $d_{s2}/D_c = 0.6$

Fig. 5 Buckling modes and k values for SS ($d_{s1}/D_c = 0.246$) and CS ($d_{s1}/D_c = 0.272$) web ($\Psi = -1.0$, $\alpha = 1.0$ and $D/t_w = 300$)

of the buckling coefficients obtained by Rockey and Cook are presented together in Table 2. The FE model considered in the present study reasonably well estimate the bend-buckling coefficients compared to the theoretical values for both the SS and CS conditions. Fig. 5(a) shows that the optimum location of the lower stiffener is $0.55D_c (= 0.275D)$ when $\Psi = -1.0$ for SS and $0.568D_c (= 0.284D)$

Table 2 Buckling coefficient values obtained from Model-I in Fig. 3 ($\Psi = -1.0$, $\alpha = 1.0$ and $D/t_w = 300$)

d_{s2}/D_c		0.52	0.54	0.55	0.56	0.568	0.60	0.64
Simply supported ($d_{s1}/D_c = 0.246$)	Model-I	278.1	304.4	312.3	304.7	298.2	270.5	234.6
	Rockey*			313.0				
Clamped ($d_{s1}/D_c = 0.272$)	Model-I	284.6	315.3	331.6	347.8	354.0	321.3	278.1
	Rockey*					356.0		

*Rockey and Cook (1965a)

when $\Psi = -1.0$) for CS conditions, that is consistent with the results of Rockey and Cook.

Fig. 5(a) shows a similar level of buckling coefficients when d_{s2}/D_c is smaller than 0.55 for SS and 0.568 for CS conditions. This is attributable to the fact that buckling occurs intensively at the lower sub-panel as shown in Fig. 5(b) in the case of $d_{s2}/D_c = 0.54$, therefore the restraint on rotation from the compression flange hardly affect the buckling strength. Meanwhile, when d_{s2}/D_c is larger than these values, buckling occurs between the compression flange and the stiffeners as shown in Fig. 5(c) in the case of $d_{s2}/D_c = 0.6$, and the CS condition exhibits larger buckling coefficients due to the restraining rotation of the upper and middle sub-panels.

The buckling coefficients obtained from a model with compression and tension flanges are also presented in Fig. 5(a) when $d_{s1}/D_c = 0.260$. The width and the thickness of the flanges were assumed to be 500 mm and 30 mm, and the corresponding compressive and tensile stresses were applied to the flanges. Fig 5(a) shows that the buckling coefficients exist between SS and CS condition of the Model-I, due to the restraining effect on the web rotation by the flanges. The SS web model will be employed for the following numerical analyses since it yields the smallest buckling coefficients.

4. Buckling analysis and proposal of buckling coefficient formula

4.1 Buckling strength under interactive in-plane bending and shear

The interactive buckling of the web panels under the concurrent action of in-plane bending and shear is studied to investigate the effect of the stiffeners on the combined buckling strength. Uniform shear stresses were applied along the edges together with the normal stresses acting as in-plane moments as shown in Fig. 3. The stress ratio $\Psi = -1$, aspect ratio $\alpha = 1$, and web slenderness ratio $D/t_w = 300$ were used. Alinia and Moosavi (2009) reported that the acceptable combinations of the maximum compressive bending stress F_c and shear stress τ are given to a close approximation by Eq. (5)

$$\left(\frac{F_c}{F_{cr}}\right)^2 + \left(\frac{\tau}{\tau_{cr}}\right)^2 = 1.0 \quad (5)$$

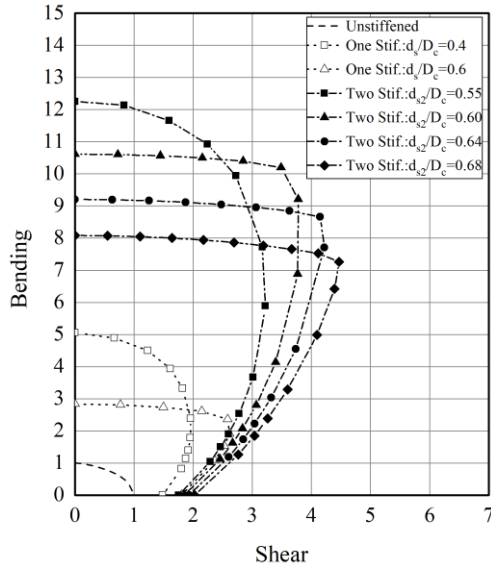


Fig. 6 Interaction diagrams for unstiffened and stiffened web panels ($d_{s1}/D_c = 0.246$, $\Psi = -1.0$, $\alpha = 1.0$, and $D/t_w = 300$)

where, F_{cr} and τ_{cr} are bend-buckling and shear buckling strengths, respectively.

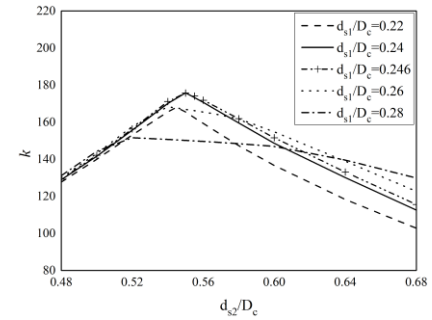
For the stiffened web with one stiffener, two cases of the stiffener location, $d_s/D_c = 0.4$ (optimum location for bend-buckling capacity) and 0.6 , were considered. For the stiffened web with two stiffeners, four cases of the stiffener locations, $d_{s2}/D_c = 0.55$ (optimum location for bend-buckling capacity), 0.60 , 0.64 and 0.68 , were considered, while d_{s1}/D_c was kept constant as 0.246 .

Based on the numerical analyses and Eq. (5), Fig. 6 shows the results for the unstiffened web and longitudinally stiffened webs, in which the buckling coefficients of the stiffened webs were normalized to that of the unstiffened case. It can be seen that, as the stiffener moves downwards from the optimum location for bend-buckling capacity, the shear buckling capacity of the plate increases consistently while the bend-buckling strength decreases, regardless of the number of stiffeners. However, the AASHTO LRFD specifications currently consider the shear buckling strength based on the unstiffened web. In addition, Fig. 6 comparatively shows that the shear buckling strengths of the web with two stiffeners increased significantly compared to those of the web with one stiffener or unstiffened web, even when the stiffeners were placed at the optimum locations for bending. Therefore, it is acceptable to determine the optimum location of the stiffeners with a focus on the maximum bend-buckling capacity.

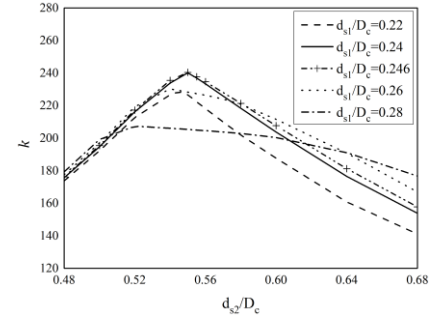
4.2 Buckling strength under in-plane bending

4.2.1 Buckling modes vs. stiffener locations

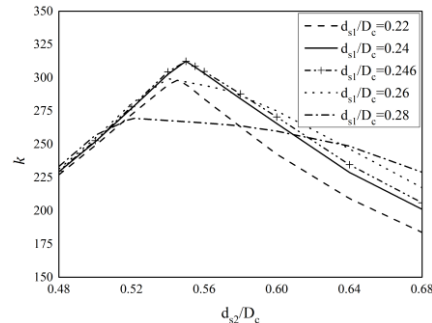
Fig. 7 collectively shows the results of the bend-buckling coefficients according to the variations of three major parameters; Ψ , d_{s1}/D_c , and d_{s2}/D_c under $\alpha = 1.0$ and $D/t_w = 300$. It is certain that the maximum buckling coefficient is obtained when $d_{s1}/D_c = 0.246$ and $d_{s2}/D_c = 0.55$, regardless of asymmetry of the cross section.



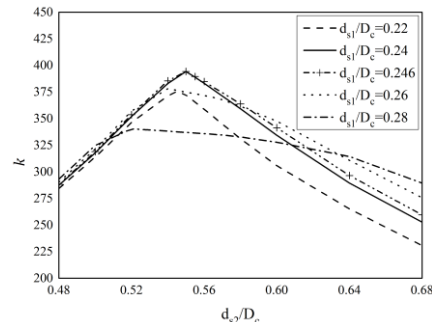
(a) $\Psi = -0.5$



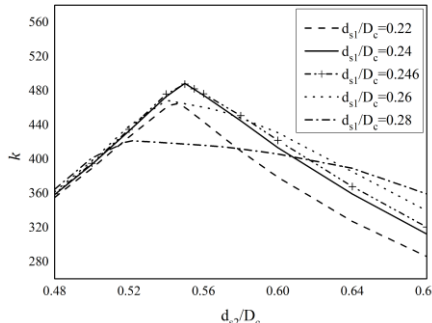
(b) $\Psi = -0.75$



(c) $\Psi = -1.0$



(d) $\Psi = -1.25$



(e) $\Psi = -1.5$

Fig. 7 Buckling coefficients vs. Ψ , d_{s1}/D_c and d_{s2}/D_c ($\alpha = 1.0$, $D/t_w = 300$)

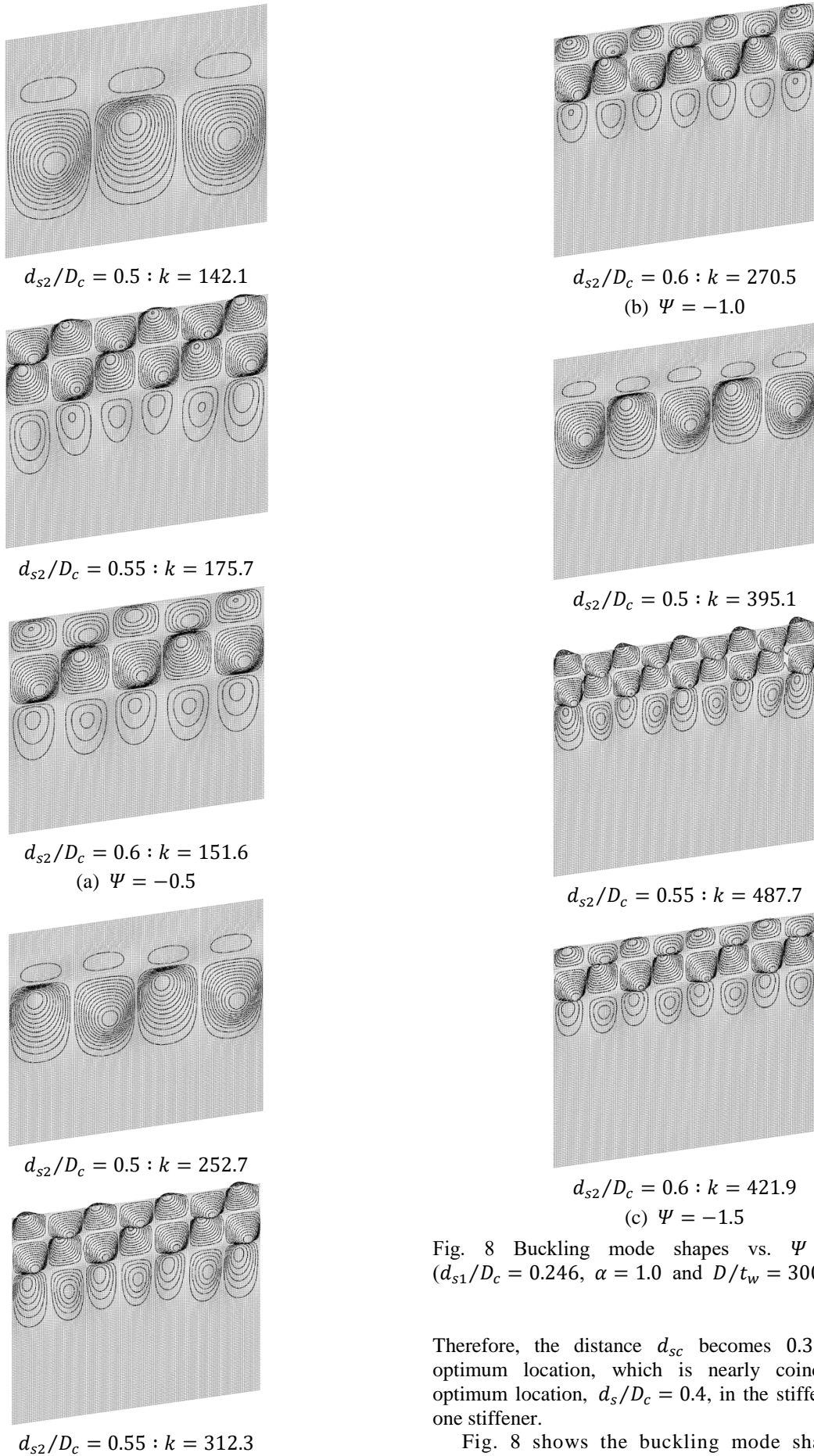


Fig. 8 Buckling mode shapes vs. Ψ and d_{s2}/D_c ($d_{s1}/D_c = 0.246$, $\alpha = 1.0$ and $D/t_w = 300$)

Therefore, the distance d_{sc} becomes $0.398D_c$ for the optimum location, which is nearly coincident to the optimum location, $d_s/D_c = 0.4$, in the stiffened web with one stiffener.

Fig. 8 shows the buckling mode shapes and the

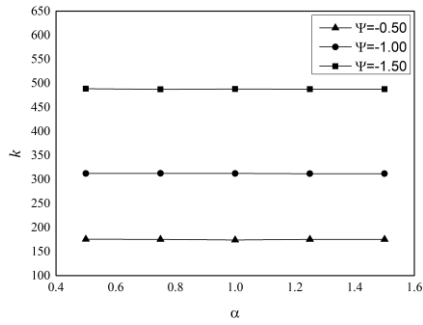


Fig. 9 Buckling coefficients vs. α ($D/t_w = 300$)

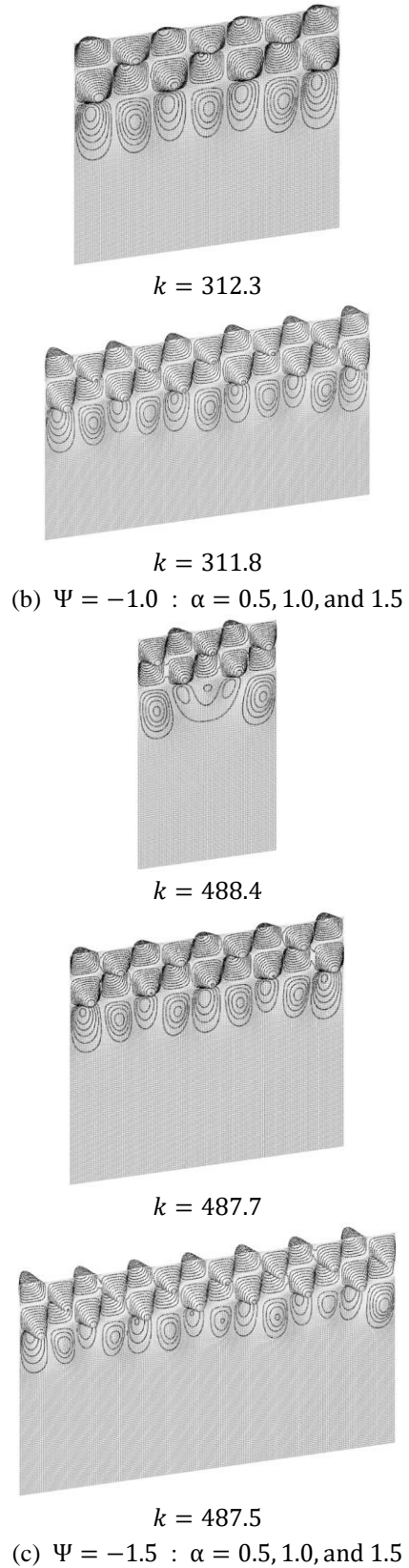
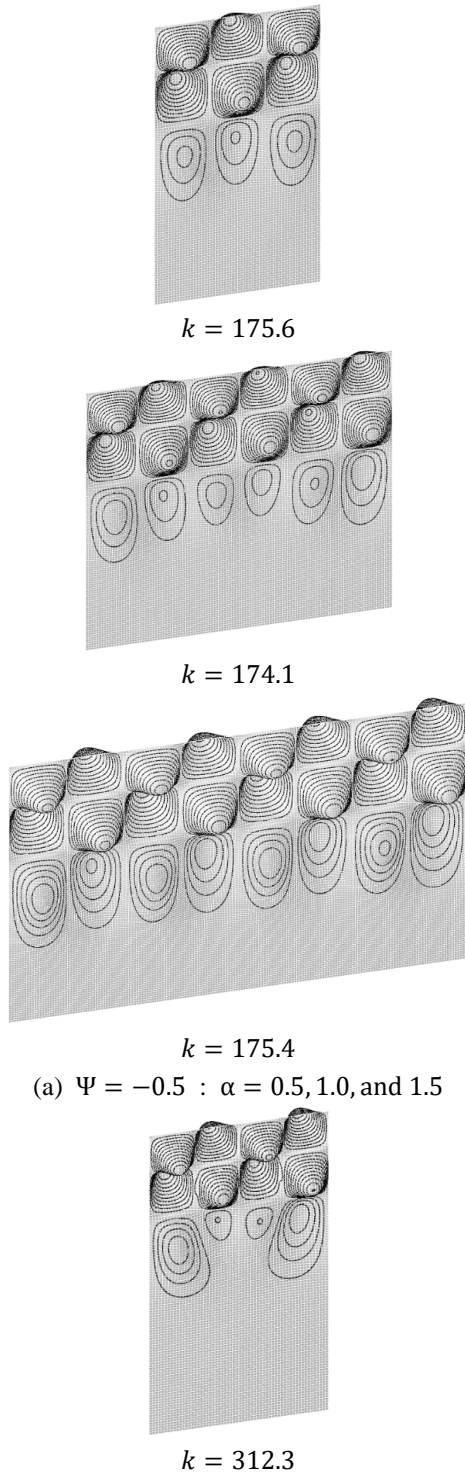


Fig. 10 Buckling mode shapes vs. Ψ and α ($d_{s1}/D_c = 0.246$, $d_{s2}/D_c = 0.55$ and $D/t_w = 300$)

corresponding buckling coefficients for the selected cases. A total of nine mode shapes in Fig. 8 represents combinations of three different stress ratios ($\Psi = -0.5$,

-1.0 and -1.5) and three different locations of the second stiffener ($d_{s2}/D_c = 0.5, 0.55, \text{ and } 0.6$) when the upper stiffener is located at $d_{s1}/D_c = 0.246$. It can be confirmed that the plate buckling occurs intensively in the lower sub-panel when $d_{s2}/D_c < 0.55$ and in the middle sub-panel when $d_{s2}/D_c > 0.55$, regardless of the asymmetry of the section. When $d_{s2}/D_c = 0.55$, anti-symmetric mode shapes with respect to the stiffener locations, i.e., simultaneous buckling are detected in all sub-panels, which results in the greatest buckling strength. In addition, the number of half-waves and the buckling coefficient increase as the stress ratio attains a smaller values under the same location ratio (d_{si}/D_c) of the stiffeners.

4.2.2 Buckling modes vs. aspect ratio

Fig. 9 shows the buckling coefficients according to aspect ratio (α) under $D/t_w = 300$. Three different stress ratios ($\Psi = -0.5, -1.0$ and -1.5) were considered, while the stiffener location parameters were set to be at the optimum locations: $d_{s1}/D_c = 0.246$ and $d_{s2}/D_c = 0.55$. Fig. 10 shows the buckling mode shapes for $\alpha = 0.5, 1.0$ and 1.5 for the three stress ratios. It is observed that the number of half-waves in the buckling mode is proportional to the aspect ratio for a specified stress ratio. This phenomenon is presumed to be related to the results that the buckling coefficients are approximately identical in Fig. 9 regardless of the aspect ratio.

4.3 Proposal of buckling coefficient formula

As confirmed in Fig. 7, the maximum bend-buckling coefficient was obtained when $d_{s1}/D_c = 0.246$ and $d_{s2}/D_c = 0.55$, regardless of the stress ratio. However, the optimum locations deviate from $d_{s2}/D_c = 0.55$ as d_{s1}/D_c varies, and then the spacing of the two stiffeners also varies. Such complex behaviors result in difficulties in deriving a consistent equation for the bend-buckling coefficients. An assumption was considered for the spacing of the stiffeners (d_{ss} in Fig. 1) by fixing it as $0.15D$, regardless of the asymmetry, which approximately corresponds to the optimum spacing $0.152D$ for $\Psi = -1.0$, i.e., doubly-symmetric section. Under this assumption, the following two cases for the stiffener locations are considered.

Case-1: The location of the stiffeners is defined using the variable d_{sc}/D_c . In this case, the locations of the upper and lower stiffeners are automatically determined from the assumption for $d_{ss}(=0.15D)$. The buckling coefficient is then dependent on the two variables, d_{sc}/D_c and Ψ . The buckling coefficients for the ranges $0.3 \leq d_{sc}/D_c \leq 0.5$ and $-1.5 \leq \Psi \leq -0.5$ are shown in Fig. 11. Fig. 11 shows that the maximum k values are obtained when $d_{sc}/D_c = 0.4$ for the range $-1.25 \leq \Psi \leq -0.5$.

Case-2: Alternatively, the location of the two stiffeners can be assumed at fixed positions, $0.125D$ and $0.275D$, regardless of the asymmetry, that are the near-optimum location in the doubly-symmetric section. In this case, the buckling coefficient is dependent only on the variable Ψ and the locations of the stiffeners are same as Case 1 when $\Psi = -1.0$. The buckling coefficients are also shown in Fig.

11 as dotted line with asterisk marks at the corresponding locations of d_{sc}/D_c , which were determined from a given Ψ .

Fig. 11 illustrates that Case-1 is more beneficial than Case-2 for the considered range of Ψ . The buckling coefficients from Case-1 shows a consistent pattern which exhibits maximum values at $d_{sc}/D_c = 0.4$ for $-1.0 \leq \Psi \leq -0.5$. By incorporating the two variables, d_{sc}/D_c and Ψ , the equation for the buckling coefficient was derived in the form of $k = 10^{m_1}(d_{sc}/D_c)^{m_2}(1 - \Psi)^{m_3}$ for $-1.0 \leq \Psi \leq -0.5$. The coefficients m_1, m_2 , and m_3 were determined based on multi-variable regression analysis (Allison 1999) and a design equation is proposed as follows

$$\begin{aligned}
 \text{Case-1: } & d_{sc}/D_c < 0.4 : k = 247.8 \left(\frac{d_{sc}}{D_c}\right)^{1.8} (1 - \Psi)^{2.7} \quad \text{for } -1.0 \leq \Psi \leq -0.5 \\
 & d_{sc}/D_c \geq 0.4 : k = 4.82 \left(\frac{D_c}{d_{sc}}\right)^{2.5} (1 - \Psi)^{2.7}
 \end{aligned} \quad (6)$$

The buckling coefficients calculated from Eq. (6) are plotted in Fig. 12 together with the numerical results from Fig. 11 for $-1.0 \leq \Psi \leq -0.5$. For the range $-1.5 \leq \Psi < -1.0$, the proposed Case-1 does not exhibits a consistent pattern as shown in Fig. 11. Fig. 11 can be used to read the buckling coefficients when the Case-1 is applied.

For the Case-2, the Eq. for the buckling coefficients was determined from curve fitting as follows.

$$\begin{aligned}
 \text{Case-2: } & \Psi < -1.0 : k = 247.8(1 - \Psi)^{0.32} \\
 & \Psi \geq -1.0 : k = 15.7(1 - \Psi)^{4.3}
 \end{aligned} \quad (7)$$

The buckling coefficients calculated from Eq. (7) are plotted in Fig. 13 together with the results from Fig. 11. In practice, Case-2 can be used for $\Psi < -1.0$ because it produces buckling coefficients larger than that of the doubly-symmetric condition. To summarize, Case-1 is recommended when $\Psi \geq -1.0$ and Case-2 when $\Psi < -1.0$.

Table 3 presents an example of the buckling coefficients for the stiffened webs by the proposed Case-1 and Case-2. For the comparison purposes, three different stress ratios, $\Psi = -0.75, -1.0$ and -1.15 , were considered, which correspond to a practical range in plate girder bridges. For the web stiffened with one stiffener, the optimum location of the stiffener, i.e., $d_s/D_c = 0.4$ was considered for the three stress ratios, and the buckling coefficient $k_{1,max}$ values were calculated from Eq. (3).

For webs with two stiffeners, Case-1 was considered for $\Psi = -0.75$ and -1.0 , and Case-2 for $\Psi = -1.15$. In Table 3, $k_{2,max}$ is the buckling coefficient obtained from the FE buckling analysis when the stiffeners are installed at the optimum locations, i.e., $d_{s1}/D_c = 0.246$ and $d_{s2}/D_c = 0.55$. Table 3 shows that the buckling coefficients of the webs with two stiffeners are more than twice as large as than those with one stiffener. It is anticipated that the buckling coefficients from the proposed methods will be about 10 ~ 12% smaller than the $k_{2,max}$ values in the practical range of Ψ . Then, the increase in D/t_w is 5 ~ 6% compared to the optimum stiffener location, which is considered acceptable in the design of plate girder bridges.

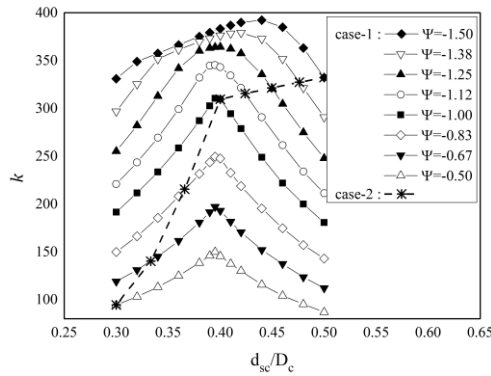


Fig. 11 Buckling coefficients for the proposed Case-1 and Case-2 ($\alpha = 1.0, D/t_w = 300$)

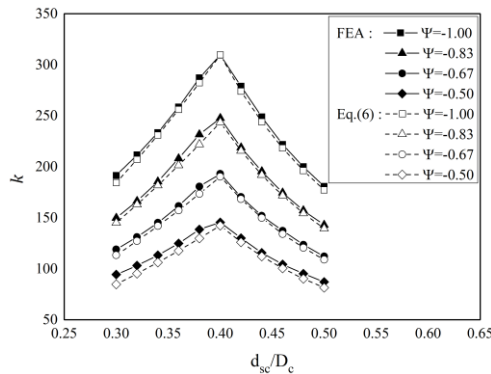


Fig. 12 Buckling coefficients from FE analysis (Fig. 11) and Eq. (6) for Case-1 ($-1.0 \leq \Psi \leq -0.5$)

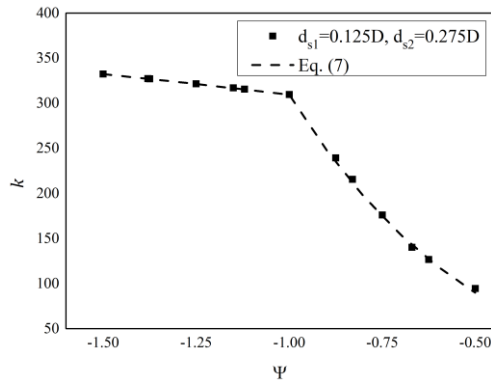


Fig. 13 Buckling coefficients from FE analysis (Fig. 11) and Eq. (7) for Case-2 ($-1.5 \leq \Psi \leq -0.5$)

Table 3 Sample comparison of buckling coefficients

Bend-buckling coefficient (k)		$\Psi = -0.75$	$\Psi = -1.0$	$\Psi = -1.15$
Web with one stiffener	$k_{1,max}$: Eq. (3)	98.9	129.3	145.3
	$k_{2,max}$: FEA	240.4	312.3	360.4
Web with two stiffener	$k_{2,max}$: Case-1: Eq. (6)	215.8	309.5	316.6
	$k_{2,max}$: Case-2: Eq. (7)			
Ratio	$k_{2,proposed}/k_{1,max}$	2.18	2.42	2.18
	$k_{2,proposed}/k_{2,max}$	0.90	0.99	0.88

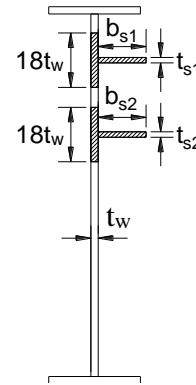


Fig. 14 Equivalent T-section

5. Rigidity of longitudinal stiffeners

5.1 AASHTO regulations and previous study on the rigidity of stiffeners

The AASHTO LRFD specifications stipulate the dimensions and the second moment of inertia for longitudinal stiffeners. The specifications limit the width-to-thickness ratio to prevent local buckling of the stiffeners as follows.

$$b_s \leq 0.48t_s \sqrt{E/F_{ys}} \tag{8}$$

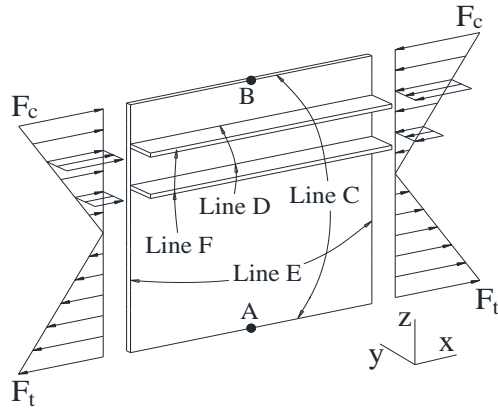
where, b_s , t_s and F_{ys} are the width, thickness and yield strength of the stiffeners, respectively.

As a rigidity requirement for longitudinal stiffeners against the out-of-plane deformation, i.e., to form ‘nodal line’ properly at the location of the stiffener, the moment of inertia of the T-section should satisfy Eq. (9), which is composed of a portion of the web corresponding to $18t_w$ and the stiffener as shown in Fig. 14.

$$I_l \geq Dt_w^3 \left[2.4 \left(\frac{d_o}{D} \right)^2 - 0.13 \right] \beta \tag{9}$$

where, I_l is the moment of inertia of the T-section with respect to its neutral axis and β is the curvature correction factor for curved girders, that is 1.0 for straight ones. It should be noted that Eq. (9) is based on the required bending rigidity of the stiffener proposed by Massonnet (1954) for webs stiffened by one line of stiffener.

Rockey and Cook (1965b) proposed an approximate equation for the required bending rigidity of stiffeners for the reinforced web with two lines of stiffeners. In their proposal, doubly-symmetric girder sections were considered and both stiffeners were assumed to have the same size. It was also assumed that the longitudinal stiffeners were doubly-sided placed about the mid-plane of the web and that the torsional rigidity was negligible. The second moment of inertia (I_l) of the double-sided stiffener with respect to the mid-plane of the web is, in general, larger than that of single-sided stiffeners with respect to its neutral axis of the T-section. However, single-sided stiffeners are usually used due to the simplicity of welding and fabrication. Therefore, this study focused on single-sided



Note: Vertical displacements (Dz) were constrained at Line F when moment-release was considered.

Fig. 15 Scheme of numerical model (Model-II) with stiffeners

stiffeners and the upper and lower stiffeners are assumed to have the same size, i.e., $b_{s1} \times t_{s1} = b_{s2} \times t_{s2}$.

5.2 Numerical analyses on the rigidity of stiffeners

5.2.1 FE model and parameters

The rigidity of each stiffener was considered in the form of a rigidity ratio (γ), which is defined as the ratio of the bending rigidity of the stiffener to that of the web as follows

$$\gamma = \frac{EI_l}{DD_{plate}} \quad (10)$$

where, $D_{plate} = Et_w^3/12(1 - \nu^2)$ is the bending rigidity of the web and ν is the Poisson's ratio ($=0.3$).

The scheme of the web model with longitudinal stiffeners is shown in Fig. 15, which will be denoted as 'Model-II'. The top and bottom junctions (Line C) and the vertical edges (Line E) were also considered as simply supported, but the out-of-plane displacements at the longitudinal stiffeners (Line D) were not constrained. The bending moment was also simulated with compressive and tensile stress gradients as shown in Fig. 15. It should be noted that the corresponding compressive stresses at the location of the stiffeners were also applied to the entire cross section of the longitudinal stiffeners. The FE mesh for the web plate was constructed in the same manner as Model-I in Fig. 3, and the stiffeners were divided so that their mesh dimensions were similar to those of the web plate.

The parameters considered for the evaluation of the required rigidity of each stiffener are the width-to-thickness ratio of the stiffener (b_s/t_s), the slenderness ratio of the web plate (D/t_w), the asymmetry of the girder section (Ψ), the aspect ratio (α), and the rigidity ratio (γ). The depth of the web (D) was also set as 3,000 mm in the subsequent analysis with the Model-II and the parameters, D/t_w , Ψ and α , were considered in the ranges in Table 1.

5.2.2 Numerical results for the width-to-thickness ratio of stiffener

Table 4 Required bending rigidity vs. b_s/t_s ($\Psi = -1.0$, $\alpha = 1.0$, and $D/t_w = 300 : D = 3,000$ mm)

Model	Size of stiffener	γ_{req}	k
Model-I (w/o stiffener)	-	-	309.4
Model-II (with stiffener)	w/o moment-release	139.8×15.5 ($b_s/t_s = 9$)	33
		140.1×14.0 ($b_s/t_s = 10$)	31
		142.6×11.9 ($b_s/t_s = 12$)	29
	with moment-release	135.8×13.6 ($b_s/t_s = 10$)	28

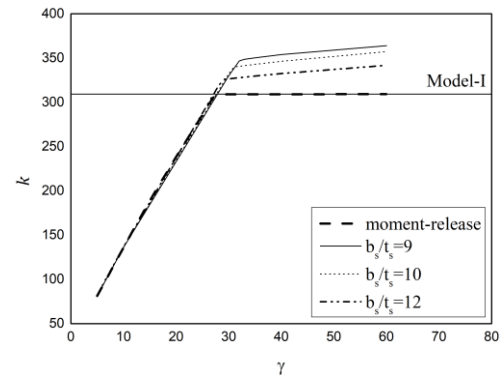
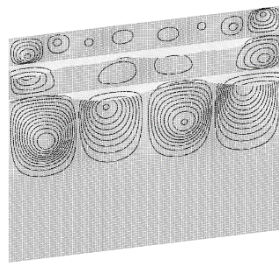


Fig. 16 Convergence curves vs. b_s/t_s ($d_{sc}/D_c = 0.4$, $d_{ss} = 0.15D$, $\Psi = -1.0$, $\alpha = 1.0$ and $D/t_w = 300$)

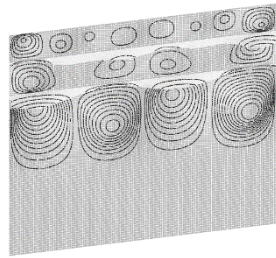
Based on Eq. (8), the stiffener with a b_s/t_s ratio of approximately 12 is typically used in the conventional steel ($F_y \leq 345$ MPa) girder bridges and the ratio will decrease as the yield strength of the steel increases. Three b_s/t_s ratios, 9, 10 and 12, were considered for the web panel under $\Psi = -1.0$, $\alpha = 1.0$ and $D/t_w = 300$. The stiffeners were placed at $d_{sc}/D_c = 0.4$ and $d_{ss} = 0.15D$ according to the Case-1.

Fig. 16 shows the convergence characteristic curves of the buckling coefficients with increase of rigidity ratio (γ) that are similar to the pattern of the 'diminishing returns curve'. The legend 'moment-release' in Fig. 16 indicates that the bending moment at the junctions of the stiffeners (Line D in Fig. 15) to the web were released to simulate the condition of zero torsional rigidity of the stiffeners. The local buckling modes by forming nodal lines were observed when the rigidity ratio, γ , reached a certain limiting point where the slope changes, also known as, the point of diminishing returns. The γ value at the point, which is the minimum rigidity ratio required for the stiffener, is denoted as γ_{req} . Table 4 presents the γ_{req} values and the corresponding k values.

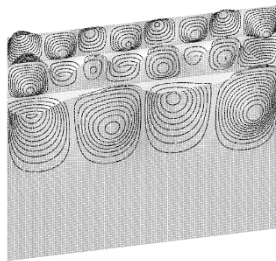
Fig. 16 shows that the models without moment-release exhibit slightly increased buckling coefficients compared to the Model-I at the limiting points, and the corresponding k values increased gradually with increasing γ . Meanwhile, the moment-release model shows the same k value by the Model-I at the limiting point and it remains constant after the point. This implies that the longitudinal stiffeners provide some restraining effects on the web rotation due to the torsional rigidity of the stiffeners. To demonstrate such



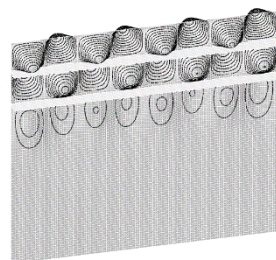
(a) $b_s/t_s = 9$



(b) $b_s/t_s = 10$



(c) $b_s/t_s = 12$



(d) $b_s/t_s = 10$: moment-release

Fig. 17 Buckling mode shapes vs. b_s/t_s ($d_{sc}/D_c = 0.4$, $d_{ss} = 0.15D$, $\Psi = -1.0$, $\alpha = 1.0$ and $D/t_w = 300$); (a), (b) and (c) without moment-release, (d) with moment-release

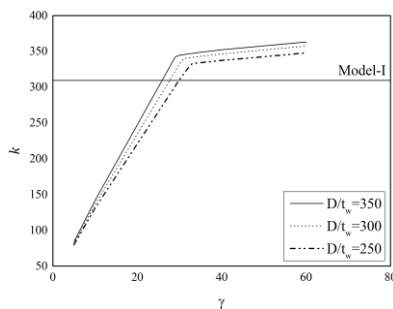


Fig. 18 Convergence curves vs. D/t_w ($d_{sc}/D_c = 0.4$, $d_{ss} = 0.15D$, $\Psi = -1.0$, $\alpha = 1.0$, and $b_s/t_s = 10$)

hypothesis, the buckling mode shapes are presented in Fig. 17 and it can be seen that the buckling of the upper and

Table 5 Required bending rigidity vs. D/t_w ($\Psi = -1.0$, $\alpha = 1.0$: $D = 3,000$ mm)

Model	D/t_w	Size of stiffener $b_s \times t_s$	$\delta (= b_s t_s / D t_w)$	γ_{req}	k
	250	162.1×16.2	0.0730	33	332.7
Model-II	300	140.1×14.0	0.0654	31	340.0
	350	123.9×12.4	0.0597	30	344.6

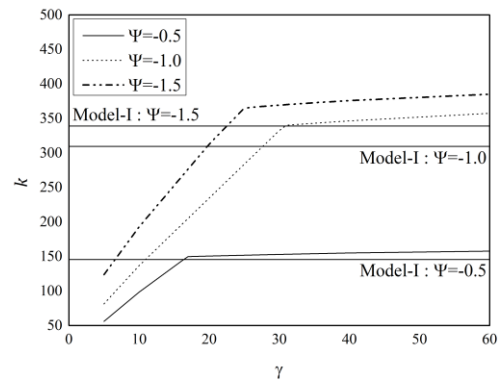


Fig. 19 Convergence curves vs. Ψ ($\alpha = 1.0$, $D/t_w = 300$ and $b_s/t_s = 10$)

middle sub-panels are gradually suppressed as the b_s/t_s ratio decreases, i.e., as the torsional rigidity increases, while the moment-release model shows the same buckling mode shape by the Model-I (See Fig. 8(b): $d_{s1}/D_c = 0.246$ and $d_{s2}/D_c = 0.55$)

Fig. 16 and Table 4 show that γ_{req} value slightly reduces as the b_s/t_s ratio increases. However, the degree of reduction in γ_{req} is not significant and the maximum b_s/t_s ratio should be controlled by Eq. (8). Therefore, the b_s/t_s ratio was assumed to be 10 and the moment-release condition was not considered in the remaining analyses.

5.2.3 Numerical results for the slenderness ratio of web plate

Three cases of $D/t_w = 250, 300$ and 350 , based on the explanation in Section 3.1, were considered to investigate γ_{req} values according to the web slenderness ratio. Fig. 18 shows the buckling coefficients with the variation of γ for the web plate with the stiffeners placed at $d_{sc}/D_c = 0.4$ and $d_{ss} = 0.15D$ under $\Psi = -1.0$ and $\alpha = 1.0$. The γ_{req} values in Fig. 18 and the corresponding k values are summarized in Table 5. It is observed from Table 5 that γ_{req} increases as the D/t_w ratio decreases. Also, γ_{req} values increase, as the area ratio (δ) increases, which is defined as the ratio of the area of the stiffener to that of the web, $b_s t_s / D t_w$. Therefore, a relationship between the variables γ_{req} and δ is expected and this will be examined in the following Section 5.3.

5.2.4 Numerical results for asymmetry of girder section

Fig. 19 shows the variation of k values with increasing γ , under $\alpha = 1.0$ and $D/t_w = 300$, for three different stress ratios ($\Psi = -0.5, -1.0$ and -1.5). For the location

Table 6 γ_{req} values vs. α and D/t_w ($d_{sc} = 0.4D_c$, $d_{ss} = 0.15D$, $\Psi = -1.0 : D = 3,000 \text{ mm}$)

aspect ratio (α)	D/t_w	size of stiffener $b_s \times t_s$	area ratio (δ)	γ_{req}
0.5	250	109.6×11.0	0.033	8.9
	300	93.1×9.3	0.029	7.9
	350	83.0×8.3	0.027	7.9
0.75	250	134.8×13.5	0.051	17.9
	300	116.7×11.7	0.046	17.0
	350	104.2×10.4	0.042	16.9
1.0	250	162.1×16.2	0.073	32.9
	300	140.1×14.0	0.065	30.9
	350	123.9×12.4	0.030	29.9
1.25	250	189.5×19.0	0.100	54.9
	300	164.5×16.5	0.090	52.3
	350	145.4×14.5	0.083	50.2
1.5	250	218.4×21.8	0.132	86.8
	300	187.5×19.0	0.119	80.4
	350	165.4×16.5	0.107	76.4

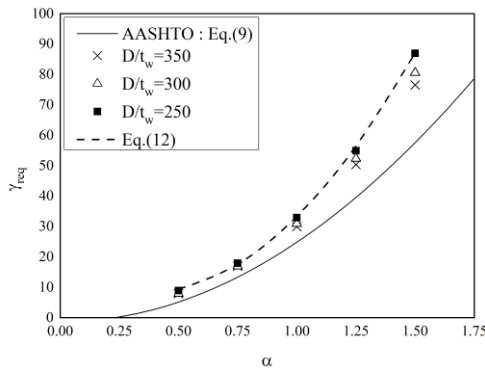


Fig. 20 γ_{req} vs. α and D/t_w ($\Psi = -1.0$, $b_s/t_s = 10$)

of the stiffeners, the Case-1 ($d_{sc}/D_c = 0.4$ and $d_{ss} = 0.15D$) was applied for the sections of $\Psi = -0.5$ and -1.0 , and the Case-2 ($d_{s1} = 0.125D$ and $d_{s2} = 0.275D$) was assumed for the section of $\Psi = -1.5$. It can also be seen that Model-II with the stiffeners yields slightly larger k values at the limiting point than the Model-I due to the torsional rigidity under all three cases. Fig. 19 shows that the maximum γ_{req} is needed for $\Psi = -1.0$ under the suggested position of the stiffeners.

5.3 Required rigidity of the stiffeners

Based on the results of the preceding parametric analysis, numerical analyses to estimate the γ_{req} values were conducted for the range of $\alpha = 0.5 \sim 1.5$ under $\Psi = -1.0$. The Case-1 was considered for the location of the longitudinal stiffeners and three different web slenderness ratios, $D/t_w = 250, 300$ and 350 , were considered.

The γ_{req} values according to the ratios, α and D/t_w ,

are summarized in Table 6 and shown in Fig. 20. The γ_{req} values calculated from the second moment of inertia of the T-section, I_l given by Eq. (9) under the AASHTO are also presented. Fig. 20 shows that γ_{req} values for the stiffener of the web reinforced with two lines of stiffeners are larger than those specified in AASHTO, which is the required rigidity when one line of the stiffener is used.

Fig. 20 also shows that γ_{req} increases as the web slenderness ratio (D/t_w) decreases and as the aspect ratio (α) increases. The γ_{req} values and the corresponding sizes of the stiffener are presented in Table 6. Based on the values in the table, an interpolation equation for the γ_{req} values were derived through the regression analysis including α and δ as variables as follows

$$\gamma_{req} = (9.0 + 55.0\delta)\alpha + (10.3 + 132.0\delta)\alpha^2$$

or

$$I_l = Dt_w^3 \left[(0.824 + 5.037\delta) \left(\frac{d_o}{D} \right) + (0.943 + 12.088\delta) \left(\frac{d_o}{D} \right)^2 \right] \quad (11)$$

A simplified equation, Eq. (12) which is derived from the web slenderness ratio $D/t_w = 250$ as the ratio is considered to be an upper bound for high-strength steel with the yield strength up to 690 MPa (100 ksi), can be used for design purposes.

$$\gamma_{req} = 59.5\alpha^2 - 41.3\alpha + 15.1$$

or

$$I_l = Dt_w^3 \left[5.45 \left(\frac{d_o}{D} \right)^2 - 3.78 \left(\frac{d_o}{D} \right) + 1.38 \right] \quad (12)$$

Eq. (12) will provide sizes of the stiffener that are on the conservative side as the web slenderness and aspect ratios increase as can be seen in Fig. 20.

6. Conclusions

The buckling strengths of stiffened webs with two lines of flat plate-shaped single-sided longitudinal stiffeners were numerically evaluated in relation to the requirements for the bending rigidity of the stiffeners. The top and bottom junctions of the web to the flanges were assumed simply supported according to the AASHTO LRFD specifications. The conclusions and recommendations proposed by this study are as follows:

1. From the interactive buckling strength analysis of web panels subjected to concurrent action of bending and shear, the stiffened webs showed highly increased shear buckling strength as well as the bend-buckling strength compared to unstiffened webs. Current AASHTO LRFD specifications evaluates shear buckling strength of stiffened webs conservatively as its strength is based on unstiffened webs. Therefore, it was considered acceptable to determine the optimum locations of the two stiffeners with focus on the maximum bend-buckling strength.

2. The numerical analyses under in-plane bending indicated that the optimum location of the upper stiffener is $0.246D_c$ and the lower stiffener $0.55D_c$, regardless of the asymmetry of the sections. Therefore, the distance d_{sc} becomes $0.398D_c$ for the optimum location, which is nearly coincident to the optimum location, $d_s/D_c = 0.4$ in the reinforced web with one stiffener.

3. A practical proposition was assumed for the spacing of the stiffeners as $0.15D$, regardless of the asymmetry, which almost corresponds to the optimum spacing of $0.152D$ in the doubly-symmetric section. This assumption was introduced to avoid changes in the optimum spacing of the stiffeners throughout the girder. Based on this assumption, two practical propositions for the location of the stiffeners were proposed, denoted as Case-1 and Case-2 in Section 4.3. The Case-1 yielded larger buckling coefficients (k) than the Case-2 for the considered range of asymmetry ratios, $-1.5 \leq \Psi \leq -0.5$. It was recommended that the Case-1 is preferable, but the Case-2 can be applicable for the range $\Psi < -1.0$ because it provides larger k values than that of the optimally placed doubly-symmetric section. Through the regression analysis for the two cases, design equations for the web bend-buckling coefficients were proposed by Eq. (6) for the Case-1 ($-1.0 \leq \Psi \leq -0.5$) and Eq. (7) for the Case-2 ($-1.5 \leq \Psi \leq -0.5$).

4. Numerical analyses on the web model with the stiffeners were conducted for the range of aspect ratio $0.5 \leq \alpha \leq 1.5$ to determine the required bending rigidity of the equivalent T-section, which is needed to form the nodal lines properly. It was found that the required rigidity is larger than that stipulated by AASHTO LRFD specifications, which is proposed for stiffened webs with one stiffener. Numerical analyses indicated that the required rigidity increases as the slenderness ratio of the web decreases. Based on the results, Eq. (11) was suggested for the bending rigidity requirement and a simplified equation, Eq. (12) was also proposed for design purposes.

Acknowledgements

This research was supported by a grant (13SCIPA01) from the Smart Civil Infrastructure Research Program funded by the Ministry of Land, Infrastructure and Transport (MOLIT) of the Government of Korea and the Korea Agency for Infrastructure Technology Advancement (KAIA).

References

- AASHTO (2017), *LRFD Bridge Design Specifications*, 8th Edition, American Association of State Highway and Transportation Officials, Washington D.C., U.S.A.
- ABAQUS (2018), *Analysis User's Manual*, v6.14, Dassault Systems, U.S.A.
- Alinia, M.M. and Moosavi, S.H. (2008), "A parametric study on the longitudinal stiffener of web panels", *Thin-Wall. Struct.*, **46**(11), 1213-1223.
- Alinia, M.M. and Moosavi, S.H. (2009), "Stability of longitudinally stiffened web plates under interactive shear and bending forces", *Thin-Wall. Struct.*, **47**(1), 53-60.
- Allison, P.D. (1999), *Multiple Regression: A Primer*, Sage Publications Ltd., London, U.K.
- Azhari, M. and Bradford, M.A. (1993), "Local buckling of I-section beams with longitudinal web stiffeners", *Thin-Wall. Struct.*, **15**(1), 1-13.
- Bleich, F. (1952), *Buckling Strength of Metal Structures*, McGraw-Hill.
- CEN (2006), *Eurocode 3: Design of Steel Structures-Part 1-5: Plated Structural Elements*, EN 1993-1-5, European Committee for Standardization, Brussels, Belgium.
- Cho, E.Y. and Shin, D.K. (2011), "Elastic web bend-buckling analysis of longitudinally stiffened I-section girders", *Int. J. Steel Struct.*, **11**(3), 297-313.
- Cooper, P.B. (1967), "Strength of longitudinally stiffened plate girders", *J. Struct. Div.*, **93**(ST2), 419-451.
- Dubas, C. (1948), "Contribution to the study of buckling of stiffened plate", Preliminary Publication, 3rd. Congress, *Int. Assoc. Bridge and Struct. Eng.*, 129.
- Frank, K. and Helwig, T.A. (1995), *Buckling of Webs in Unsymmetric Plate Girders*, Engineering J., Second Quarter, 43-53.
- Issa-El-Khoury, G., Linzell, D.G. and Geschwindner, L.F. (2014), "Computational studies of horizontally curved, longitudinally stiffened, plate girder webs in flexure", *J. Constr. Steel Res.*, **93**, 97-106.
- Kim, H.S., Park, Y.M., Kim, B.J. and Kim, K. (2018), "Numerical investigation of buckling strength of longitudinally stiffened web of plate girders subjected to bending", *Struct. Eng. Mech.*, **65**(2), 141-154.
- Maiorana, E., Pellegrino, C. and Modena, C. (2011), "Influence of longitudinal stiffeners on elastic stability of girder webs", *J. Constr. Steel Res.*, **67**(1), 51-64.
- Massonnet, C. (1954), *Essais de Voilement sur Poutres à Âme Raidie*, Publications, Int. Assoc. Bridge and Struct. Eng., Zurich, Switzerland.
- Park, Y.M., Lee, K.J., Choi, B.H. and Cho, K.I. (2016), "Modified slenderness limits for bending resistance of longitudinally stiffened plate girders", *J. Constr. Steel Res.*, **122**, 354-366.
- Rockey, K.C. (1958), "Web buckling and the design of web-plates", *Struct. Eng.*, **36**(2), 45-60.
- Rockey, K.C. and Leggett, D.M.A. (1962), "The buckling of a plate girder web under pure bending when reinforced by a single longitudinal stiffener", *Proc. Inst. Civil Eng.*, **21**(1), 161-188.
- Rockey, K.C. and Cook, I.T. (1965a), "Optimum reinforcement by two longitudinal stiffeners of a plate subjected to pure bending", *Inst. J. Sol. Struct.*, **1**(1), 79-92.
- Rockey, K.C. and Cook, I.T. (1965b), "The buckling under pure bending of a plate girder reinforced by multiple longitudinal stiffeners", *Inst. J. Sol. Struct.*, **1**(2), 147-156.
- Timoshenko, S.P. and Gere, J.M. (1963), *Theory of Elastic Stability*, McGraw-Hill.
- Zieman, R.D. (2010), *Guide to Stability Design Criteria for Metal Structures*, 8th Edition, John Wiley & Sons.

Notations

		ν	Poisson's ratio of steel
A_{fc}	area of the compression flange	ψ	stress ratio in the web panel
A_{ft}	area of the tension flange		
A_s	area of the longitudinal stiffener		
b_s	projecting width of the longitudinal stiffener		
D	web depth		
D_c	depth of the web in compression in the elastic range		
D_{plate}	bending rigidity of the web plate		
d_o	spacing of the transverse stiffeners		
d_{si}	distance between the i^{th} longitudinal stiffener and the inner surface of the compression flange		
d_{sc}	distance between the center of the two longitudinal stiffeners and the inner surface of the compression flange		
d_{ss}	distance between the upper longitudinal stiffener and the lower longitudinal stiffener		
E	elastic modulus of steel		
F_c	compressive stress on the top of the web		
F_{crw}	nominal web bend-buckling resistance		
F_t	tensile stress on the bottom of the web		
F_{yc}	yield strength of the compression flange		
F_{ys}	yield strength of the longitudinal stiffener		
I_l	moment of inertia of the T-section with respect to its neutral axis		
k	elastic web bend-buckling coefficient		
t_{si}	thickness of the i^{th} longitudinal stiffener		
t_w	web thickness		
α	aspect ratio of the web panel		
γ	rigidity ratio of the stiffener to the web plate		
δ	cross sectional area ratio of the longitudinal stiffener to the web plate		
τ	shear stress		